Structural investigation of the ternary alloys system a-GaAsP and correlation with optical properties

1992 J. Phys.: Condens. Matter 4 2817

(http://iopscience.iop.org/0953-8984/4/11/010)

J. Phys.: Condens. Matter 4 (1992) 2817–2829. Printed in the UK

Structural investigation of the ternary alloy system a-GaAsP and correlation with optical properties

S H Baker†, M I Manssor†, S J Gurman†, S C Bayliss‡ and E A Davis†

† Department of Physics and Astronomy, University of Leicester, Leicester LE1 7RH, UK

‡ Department of Physics, Loughborough University of Technology, Loughborough, Leicestershire, UK

Received 14 November 1991

Abstract. Amorphous GaAsP (a-GaAsP) films have been prepared by radiofrequency sputtering in argon. The composition in the deposited films was altered by varying the number of phosphorus pieces added to a crystalline GaAs target. The local structure and bonding configurations in the films have been investigated using extended x-ray absorption fine-structure (EXAFS) techniques. EXAFS spectra have been recorded at the K edges of each constituent element, and this has allowed us to construct a reasonably detailed picture of the local structure in the a-GaAsP films. The results of optical absorption and infrared measurements are also reported and are found to correlate well with the EXAFS measurements.

1. Introduction

Over the past 20 years or so, a great deal of fundamental and applied research has taken place in the field of amorphous semiconductors; in particular, much effort has been directed towards amorphous silicon (a-Si) and its associated alloys, e.g. a-SiN_x, a-$Si_{1-x}C_x$. Far less is known about amorphous III–V semiconductors, although there have been numerous studies on the corresponding crystalline materials in view of their many applications. For example, the high carrier mobility of GaAs has led to its use in fast electronic devices. The band gaps of ternary III–V alloys such as $Ga_{1-x}Al_xAs$ and $GaAs_{1-x}P_x$ may be 'tuned' simply by altering the composition x; these materials are now widely used in optoelectronic devices. Recently, reports suggest that amorphous III–V semiconductors may have potential applications as optical storage media [1]. One might therefore anticipate an increased applied and fundamental interest in these materials.

The majority of previous work on amorphous III–V alloys is concerned with a-GaAs. From extended x-ray absorption fine-structure (EXAFS) measurements [2], and also optical [3] and electron diffraction experiments [4], Theye and co-workers suggested that the structure of stoichiometric flash-evaporated a-GaAs was reasonably well chemically ordered, with few wrong bonds, i.e. few Ga–Ga and As–As bonds. Recently, EXAFS measurements have been used by Baker *et al* [5] to investigate the local structure in sputtered a-$Ga_{1-x}As_x$, where x was varied between 0.5 and 0.85. The extension of measurements to As-rich films revealed that, while Ga atoms remained tetrahedrally coordinated throughout the composition range studied, the As coordination decreased

0953-8984/92/112817 + 13 $04.50

from 4 at stoichiometry towards 3 (the coordination expected in a-As) as x was increased from 0.5 towards 1. Changes in the infrared spectra of the a-$Ga_{1-x}As_x$ films with increasing x also suggested that the As bonding environment changed from being predominantly like that in GaAs around stoichiometry to one more like that in a-As for As-rich films.

There are hardly any reports in the literature on amorphous ternary III–V alloys, although Manssor and Davis [6] have recently investigated optical and electrical properties of a-GaAlAs. In this study, we have investigated the local structure and bonding configurations in a-GaAsP as a function of composition, by means of EXAFS techniques. The results of optical (visible and infrared) absorption measurements are also presented and are correlated with the EXAFS data. The EXAFS results, in particular, indicate that the bonding environment around Ga atoms is partially ordered, with Ga–P bonding maximized.

2. Specimen preparation

The a-$Ga_xAs_yP_z$ samples were prepared by radiofrequency (RF) sputtering in an argon atmosphere at a pressure of ~4 mTorr. Before admitting the sputtering gas, the system was evacuated to a base pressure of 2×10^{-7} mTorr or better. The films were sputtered from a crystalline GaAs target, to which pieces of red phosphorus were added. A power of 75 W was supplied to the target at a frequency of 13.56 MHz. The films were deposited at a temperature of 15–20 °C onto various substrates: Corning 7059 for optical work, crystalline Si for infrared spectroscopy, copper foil and Mylar for EXAFS measurements and aluminium foil for composition determination.

The composition of the films was altered by varying the number of pieces of phosphorus added to the target, and was determined by energy-dispersive x-ray analysis (EDAX). In all cases, the Ga and As concentrations were approximately equal, i.e. $x \simeq y$, while the P content varied between 14 and 73 at.%. In other words, the sample compositions can be represented as

$$\text{a-}(GaAs)_{0.5(1-z)}P_z$$

where $0.14 \leqslant z \leqslant 0.73$. This is, of course, not directly analogous to the crystalline case, where the composition is given by

$$Ga_{0.5}As_{0.5-x}P_x$$

3. Experimental details

The EXAFS measurements on the a-GaAsP films were carried out using the 2 GeV synchrotron radiation source at the SERC Laboratory at Daresbury. Beam currents during data-taking were between 150 and 250 mA.

The phosphorus K-edge data were obtained on station 3.4 (SOXAFS). This has a Cr-plated mirror, which focuses the beam at the sample. The mirror also has a high-energy reflectivity cut-off at about 3.5 keV so that harmonic contamination of the monochromatic beam is minimal. The energy of the x-ray beam reaching the sample was defined by an InSb double-crystal monochromator, the incident flux being monitored by an Al foil. Absorption at the sample was measured by the electron drain current method,

a modification of the total electron yield technique. This method measures the electron drain needed to earth the sample after electron emission; hence, the amorphous films were deposited onto copper substrates for these experiments.

The Ga and As K-edge data were obtained on station 7.1, which has a Si(1 1 1) double-crystal monochromator. Harmonic rejection was set at 70% by detuning the monochromator. The x-ray absorption was measured using standard transmission geometry, with incident and transmitted fluxes measured by ionisation chambers containing an Ar–He gas mixture. Samples deposited on thin low-absorbing Mylar substrates were used for these measurements; in order to obtain the necessary sample thickness, several layers were stacked together.

The EXAFS spectra were extracted from the measured absorption spectra using the standard Daresbury program EXBACK [7]. These were analysed by a least-squares curve-fitting technique, implemented in the Daresbury program EXCURV88 [7]. This program uses the fast curved-wave theory [8], the required electron scattering phaseshifts being calculated within the program. The program also contains a statistics package that gives the uncertainties on the (often strongly correlated) structural parameters [9]. The uncertainties we quote are always the limits of the 95% confidence region, i.e. the $\pm 2\sigma$ uncertainties. The structural parameters fitted were the type and number N_j of scattering atoms at a distance r_j, the mean square deviation in r_j, σ_j^2 (the Debye–Waller factor), and the energy offset E_0. The overall amplitude parameter and the electron mean-free-path parameter were determined by a study of the EXAFS from a sample of crystalline GaAs, which was also used to check the phaseshifts. All of these parameters are fully described in our earlier work [10].

Infrared transmission spectra for the a-GaAsP films were recorded using a Perkin–Elmer 580 spectrophotometer. The chamber containing the sample holder was purged thoroughly with dry air in order to reduce absorption due to water vapour.

At visible and near-infrared photon energies, the optical absorption α was measured by conventional transmission and reflection methods on a Perkin–Elmer 330 spectrophotometer. Values for the optical band gap E_{opt} were deduced by fitting α to the Tauc relation

$$(\alpha\hbar\omega)^{1/2} = B(\hbar\omega - E_{opt})$$

where $\hbar\omega$ is the photon energy and B is a (composition-dependent) constant.

4. Results of extended x-ray absorption fine-structure study

Figure 1 gives examples of the background-subtracted EXAFS functions $\chi(k)$, weighted by k^3 or k^2, and their associated Fourier transforms. As always with EXCURV88 output, the Fourier transforms are phase-corrected so that the peaks appear at the true interatomic distances. In most cases described here, the noise level was sufficiently low to allow data out to $k \simeq 12$–13 Å^{-1} to be used. The absence of second- or higher-neighbour contributions to any of the Fourier transforms confirms the amorphous nature of our films.

A major problem with the analysis of the data from our samples is that Ga and As, since they are very close in atomic number, have very similar backscattering amplitudes and phaseshifts. It is consequently impossible to distinguish between Ga and As scatterers. We have therefore assumed that around each absorbing Ga, As or P atom, there may be two atom types, P or X, where X denotes either a Ga or an As atom.

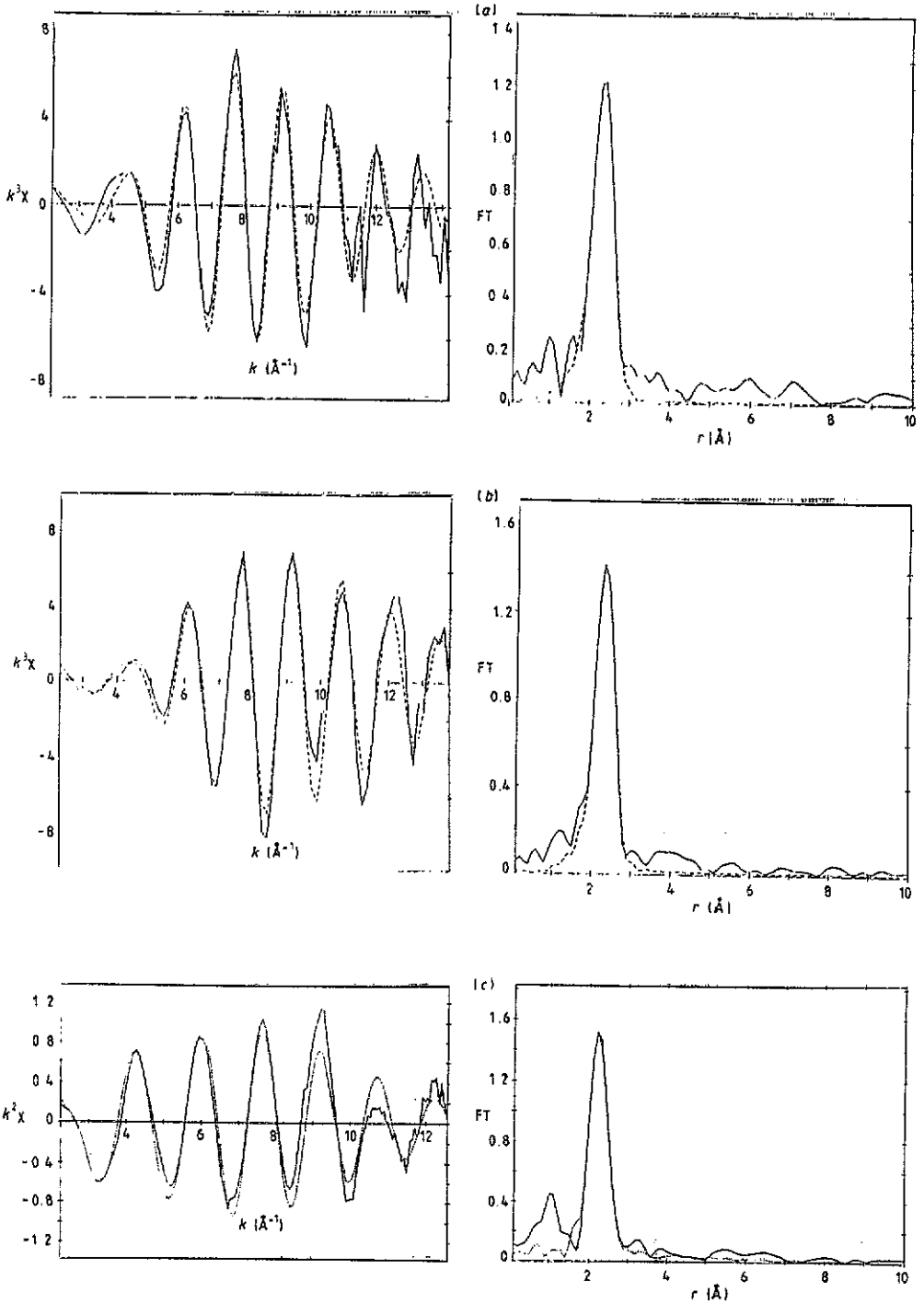

Figure 1. EXAFS spectra χ (k^3-weighted in the case of the Ga and As K-edge spectra, k^2-weighted for the P K-edge spectrum) and their associated Fourier transforms (FT): (*a*) Ga K edge $k^3\chi$ and FT for sample containing 14 at.% P. (*b*) As K edge $k^3\chi$ and FT for sample containing 46 at.% P. (*c*) P K edge $k^2\chi$ and FT for sample containing 73 at.% P. The full curves represent the experimental data; the broken curves give the least-squares fit.

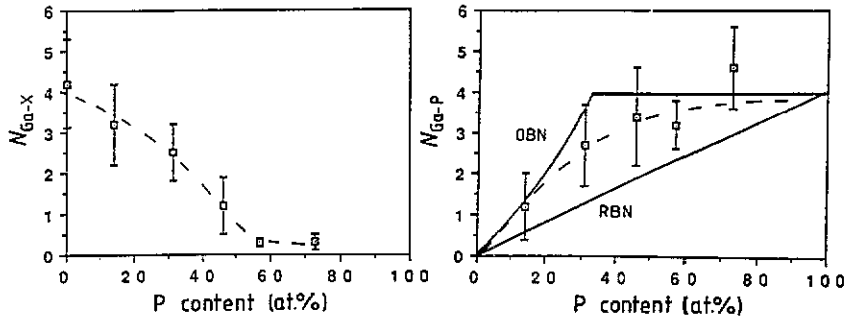

Figure 2. Partial Ga coordinations N_{Ga-X} and N_{Ga-P} as a function of composition. The broken curves in this and subsequent figures are drawn as guides to the eye.

Changing X from Ga to As or vice versa always altered the fitted structural parameters by much less than their uncertainties.

The EXAFS data for crystalline GaAs gave bond lengths of 2.43 ± 0.02 Å (Ga edge) and 2.42 ± 0.02 Å (As edge), and coordinations of 4.0 ± 0.5 for each when the amplitude factor was set at 0.7 and the mean-free-path parameter V_i at −3 eV. The two sets of scattering parameters give consistent results but both give slightly short distances; the standard bond length for c-GaAs is 2.45 Å. This points towards a small error in the phaseshifts used in the data analysis but does not, however, affect the conclusions drawn in this study.

All of the bond lengths determined by our analysis were found to be independent of composition within their uncertainties. The values found were $r_{Ga-X} = 2.42$ Å, $r_{As-X} = 2.42$ Å, $r_{Ga-P} = 2.33$ Å, $r_{As-P} = 2.31$ Å, $r_{P-X} = 2.35$ Å and $r_{P-P} = 2.20$ Å (all ±0.02 Å), as determined from the EXAFS on the absorption edge of the first-named atom. For comparison, we note that the bond lengths in (crystalline) c-GaP, a-As and c-P (black) are 2.36 Å, 2.45–2.48 Å [11] and 2.18 Å. Values reported for the Ga–Ga bond length are 2.76 Å in amorphous metallic Ga [12] and 2.48 Å for dimers in crystalline orthorhombic Ga [13]. The sum of the covalent radii of As and P is 2.28 Å. The close similarity of our measured bond lengths to those of stoichiometric materials and their invariance as functions of composition strongly suggest that the covalent bonds are well defined and unchanging entities in our amorphous films.

The measured mean-square variations in bond length (the Debye–Waller factors) are very similar for all of the bond types in the amorphous network, with $\sigma^2 = 0.006 \pm 0.001$ Å^2. They vary little with composition and the two values of σ^2 for the same bond, deduced from different edge measurements, are always consistent. An Einstein model calculation, using vibrational frequencies of 250 cm^{-1} for Ga–As bonds and 350 cm^{-1} for Ga–P bonds (see section 5), gives thermal contributions to σ^2_{Ga-As} and σ^2_{Ga-P} of 0.005 Å^2 and 0.006 Å^2 respectively. For c-GaAs, where it is assumed that σ^2 has only a thermal contribution, we found that $\sigma^2 = 0.005 \pm 0.001$ Å^2. There is therefore very little structural disorder in the bond length. This is a common finding in amorphous materials; long-range order is destroyed by bond-angle variation (hence the absence of a second-neighbour contribution to our spectra).

The measured partial coordination numbers and their $\pm 2\sigma$ uncertainties are shown in figures 2–7 together with the total coordination numbers for each atom type, obtained by summing the partials. Figure 2 shows the partial Ga coordinations N_{Ga-X} and N_{Ga-P} as functions of P content. (The Ga and As contents are almost equal for all samples.)

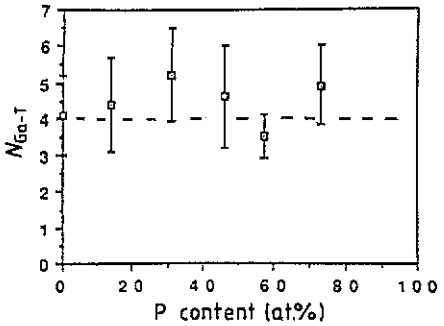

Figure 3. Total Ga coordination N_{Ga-T} as a function of composition.

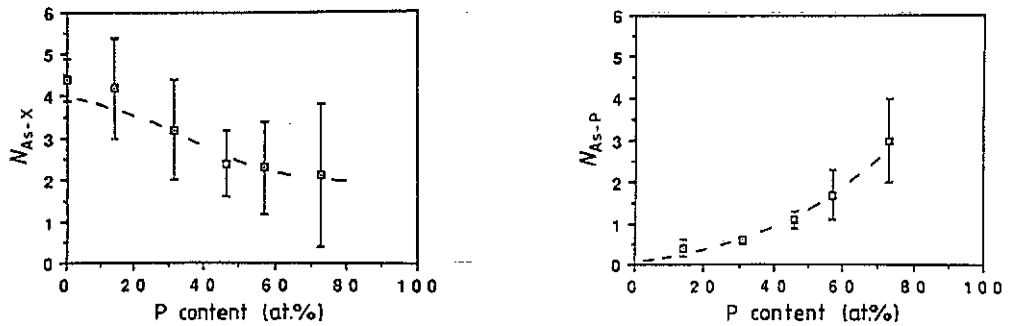

Figure 4. Partial As coordinations N_{As-X} and N_{As-P} as a function of composition.

As the P content increases, N_{Ga-P} clearly increases rapidly and maximizes at the expense of Ga–X (presumably mainly Ga–As) bonding. The total Ga coordination N_{Ga-T} remains consistent with 4 across the composition range, as can be seen from figure 3. Also shown on figure 2 are the predictions of two simple bond models for tetrahedrally coordinated Ga: an ordered bond network (OBN) model in which the number of Ga–P bonds is maximized, and a random bond network (RBN) model in which the bonding is statistical. These are the limiting cases of a more general model [14]. We can see that the Ga environment in the a-GaAsP films appears to be at least partially ordered, with Ga–P bonds favoured.

The partial As coordinations N_{As-X} and N_{As-P} are given in figure 4. It is evident that N_{As-P} rises more slowly with increasing P content than N_{Ga-P}. Consequently, N_{As-X} decreases fairly gradually as the P content is increased. It is interesting to note that for P contents greater than about 50 at.%, N_{As-X} is appreciably greater than N_{Ga-X}. From figure 2, we know that in very P-rich films Ga atoms are almost completely coordinated by P atoms. Also, since the contents of Ga and As in these films are equal, N_{Ga-As} must equal N_{As-Ga} for bond consistency. Therefore, at very high P content (>50 at.%) there must be some As–As bonding. This does not show up in the distance measurement since the As–As bond length is greater than the Ga–As bond length by only 0.00–0.03 Å (within the error of the measurement). It should be noted that As atoms appear to be tetrahedrally coordinated at all compositions, as can be seen from figure 5, which shows the total As coordination N_{As-T}. If there is an appreciable amount of As–As bonding

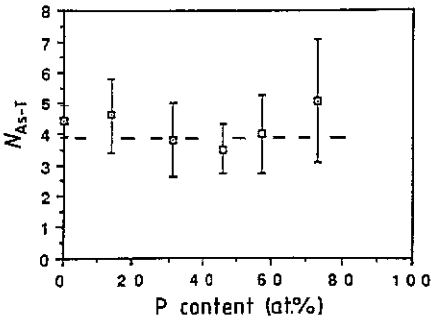

Figure 5. Total As coordination N_{As-T} as a function of composition.

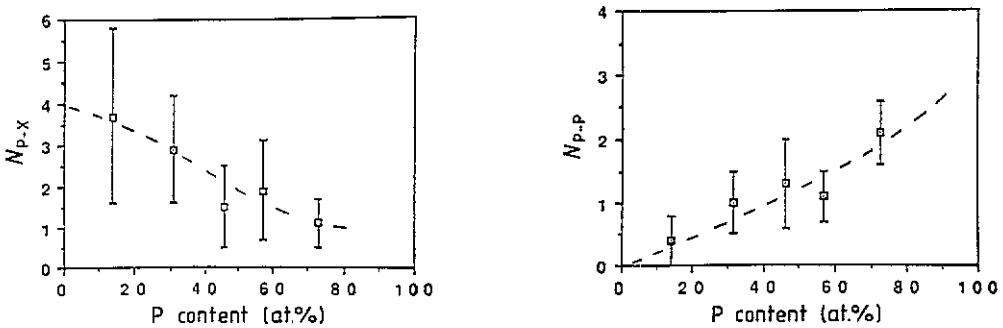

Figure 6. Partial P coordinations N_{P-X} and N_{P-P} as a function of composition.

(relative to As–Ga bonding) in very P-rich samples, one might expect the measured value of N_{As-T} to fall towards 3 (its value in a-As) at the P-rich end of the composition range. Any such trend would be masked by the large size of our uncertainties.

In figure 6, the P partial coordinations N_{P-P} and N_{P-X}, determined from the EXAFS on the P K edge, are given as functions of composition. As might be expected in samples whose composition is given essentially by $(GaAs)_{0.5(1-z)}P_z$, N_{P-P} increases with rising P content, although the rate at which this occurs is fairly gradual; N_{P-X} shows a steady decrease. From figures 2 and 4, we have already seen that Ga–P bonds outnumber As–P bonds; the N_{P-X} values plotted in figure 6 therefore refer mostly to P–Ga bonds. We may use a simple bond consistency condition to show that P–Ga bonds outnumber P–As bonds by about 3:1 for almost all compositions; this point is further considered below. The total P coordinations N_{P-T} are given in figure 7. There is some suggestion of a decrease in N_{P-T} from 4 at low P content towards 3 in P-rich films. Although the size of the error bars ($\sim\pm1$) prevents us, strictly speaking, from being definite about this, a coordination of 3 in a–P would indicate the likelihood of such a trend. The data in figure 7 suggest that P atoms are predominantly tetrahedrally bonded up to ~30 at.% P (almost the equiatomic composition). Since Ga and As atoms are 4-fold coordinated across the composition range studied, the amorphous network therefore appears to be predominantly tetrahedrally bonded for P contents up to 30 at.% or so. Beyond this, the decrease in N_{P-T} towards 3 indicates a network of mixed 4-fold and 3-fold coordination. As has already been pointed out in section 1, a somewhat similar situation was found by

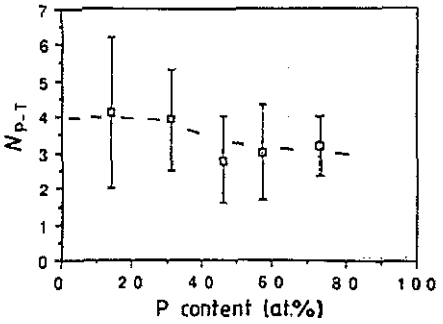

Figure 7. Total P coordination N_{P-T} as a function of composition.

Table 1. Comparison of partial coordinations.

Composition (at.%)			Measured		Calculated			Measured	
x	y	z	N_{Ga-P}	N_{As-P}	N_{P-Ga}	N_{P-As}	Sum	N_{P-X}	N_{P-P}
14	13	73	4.6 ± 1.0	3.0 ± 1.0	0.9 ± 0.2	0.5 ± 0.2	1.4 ± 0.3	1.1 ± 0.6	2.1 ± 0.5
21	22	57	3.2 ± 0.6	1.7 ± 0.6	1.2 ± 0.2	0.7 ± 0.2	1.9 ± 0.3	1.9 ± 1.2	1.1 ± 0.4
28	26	46	3.4 ± 1.2	1.1 ± 0.2	2.1 ± 0.7	0.6 ± 0.1	2.7 ± 0.7	1.5 ± 1.0	1.3 ± 0.7
36	33	31	2.7 ± 1.0	0.6 ± 0.1	3.1 ± 1.2	0.6 ± 0.1	3.7 ± 1.2	2.9 ± 1.3	1.0 ± 0.5
46	40	14	1.2 ± 0.8	0.4 ± 0.2	3.9 ± 2.6	1.1 ± 0.6	5.0 ± 2.7	3.7 ± 2.1	0.4 ± 0.4
49	51	0							

the present authors in a-$Ga_{1-x}As_x$ [5], with Ga atoms remaining 4-fold coordinated but with the As coordination decreasing towards 3 as the films became increasingly As-rich.

It is possible to check for consistency between the coordination numbers determined from the different absorption edge measurements by means of a simple bond-counting argument. We simply argue that the number of A–B bonds in a sample must be the same whether viewed from an A or a B atom. This gives us a constraint on the partial coordination numbers, which may be written as

$$c_A N_{A-B} = c_B N_{B-A}$$

where c_i is an atomic concentration and N_{i-j} is a partial coordination (the number of j atoms bonded to each i atom). The inability to distinguish Ga and As scatterers limits the applicability of this equation in the present case, although we can use it for bonds involving a P atom. We first use the above equation to calculate N_{P-Ga} and N_{P-As} from the partial coordinations N_{Ga-P} and N_{As-P}, which were determined from the Ga and As edge data. We then compare the sum of these to the partial coordination N_{P-X} determined from the P edge data. The results are given in table 1.

First, we note that all values of N_{P-X} are consistent within their uncertainties. Thus, we may have some confidence in our coordination numbers. We also note that the number of P–Ga bonds is much greater than the number of P–As bonds; the ratio is about 3:1 at low P content, falling only to about 2:1 at the highest P content. It should also be pointed out that the number of P–Ga bonds is greater than the number of P–P bonds until the P content reaches 60–70 at.% (where the Ga content is only 15–20 at.%). We shall return to this point in section 7.

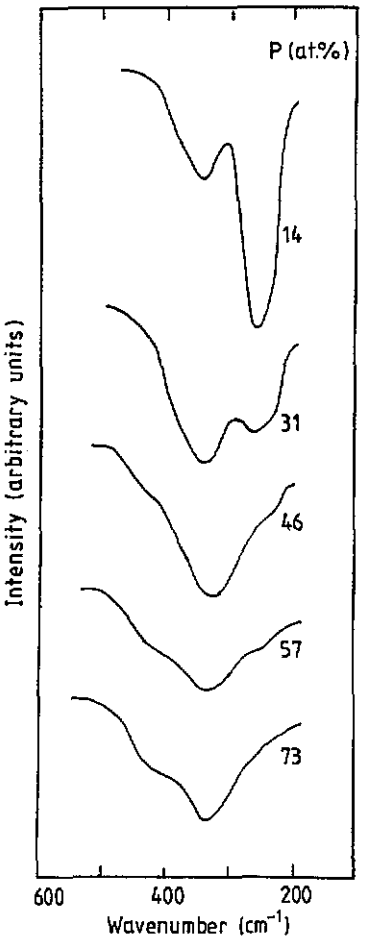

Figure 8. Infrared transmission spectra for the a-GaAsP films.

5. Results of infrared study

The infrared transmission spectra for a-GaAsP films prepared at the same time as those used for EXAFS results are shown in figure 8. The two main features that can be observed are absorption modes at ~250 and ~350 cm^{-1}. These correspond to the TO normal modes in a-GaAs and a-GaP respectively and may be assigned to Ga–As and Ga–P bond stretching vibrations. Both are broadened and shifted to lower wavenumber from the respective crystal values of 268 cm^{-1} in c-GaAs and 366 cm^{-1} in c-GaP.

Even in the sample containing least phosphorus, the GaP-related mode is very clear, indicating a significant content of Ga–P bonds. The rapid growth of this mode with increasing P content, and the sharp decrease of the GaAs-related mode, mirrors the bond proportions obtained from the EXAFS data. It should be noted that the GaAs-related mode is almost completely absent for P contents over 50 at.%.

An additional feature for samples with high P contents is the increased absorption between about 400 and 500 cm^{-1}, which appears to broaden the GaP TO mode on the higher-wavenumber side and, in the case of the most P-rich samples, gives rise to a

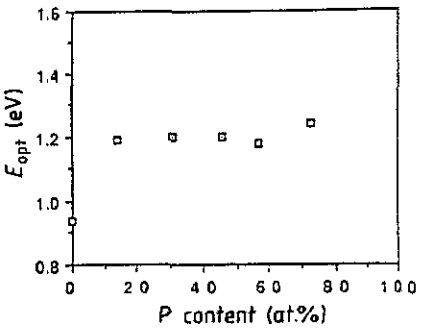

Figure 9. Optical gap E_{opt} for the a-GaAsP films as a function of composition.

clearly visible shoulder. This could be due to the presence of P–P bonds, since a–P is known to be infrared-active in this region [15].

6. Optical absorption results

Figure 9 shows the optical band gap E_{opt}, deduced from measurements of optical absorption α (as described in section 3), as a function of composition for a-GaAsP films prepared in the same deposition run as those for EXAFS and infrared measurements. At zero P content, i.e. for a-GaAs, E_{opt} is approximately 0.94 eV, which agrees reasonably with previous work [3, 5, 6]. The error in E_{opt} is ± 0.02 eV. As P is introduced into the amorphous network, there is initially quite a sharp increase in E_{opt} to around 1.2 eV; it remains at this value with increasing P content up to about 60–70 at.% P, above which there are signs of a further increase in E_{opt}.

Gheorghiu and Theye [3] have reported a figure of 1.2 eV for the optical gap in stoichiometric a-GaP, with somewhat larger values in P-rich samples. The constancy of E_{opt} for the a-GaAsP films over an appreciable composition range, and at a value characteristic of a-GaP, could be interpreted as due to the dominant contribution of Ga–P bonds and so consistent with the EXAFS data. The rapid rise of E_{opt} at low P contents is, on this picture, due to the rapid replacement of Ga–As bonds by Ga–P bonds (see figure 2). However, as we shall see in section 7, some caution is required with this argument. For the most P-rich sample, it should be noted that, although E_{opt} is greater than 1.2 eV, it is still considerably less than 1.75 eV, the optical gap in a-P [15].

7. Discussion

The EXAFS and infrared data described in sections 4 and 5 provide a consistent picture of the bonding in the a-GaAsP thin films. Our results show that Ga–P bonds are favoured, the Ga–P coordination increasing rapidly with P content. Consequently, N_{Ga-X} falls sharply, becoming close to zero at 50 at.% P. As a further consequence, there is a good deal of As–As coordination at high P content. N_{P-P} rises only slowly until the P content is greater than about 50 at.%.

A discussion of the structure of these materials, and therefore any interpretation of their properties in terms of their structure, is hampered by the inability to distinguish Ga and As scattering atoms. In order to be more definite, we shall *assume* in this section

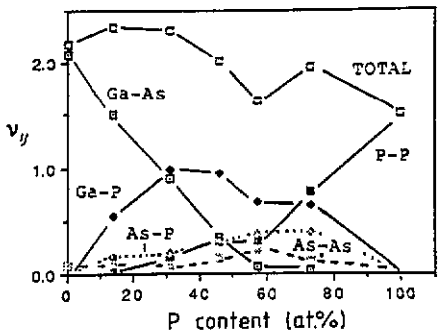

Figure 10. Bond numbers ν_{ij} as a function of composition for the various bond types (assuming no Ga–Ga bonds).

that there are no Ga–Ga bonds in the films. There is certainly no contribution around 2.76 Å, the bond length in amorphous metallic gallium [12], but the EXAFS data cannot rule out a contribution from Ga–Ga at 2.48 Å, the dimer bond length in orthorhombic Ga [13].

With the *assumption* of no Ga–Ga bonds, $N_{\text{Ga-X}}$ becomes $N_{\text{Ga-As}}$ and we have the three partial Ga coordinations. Use of the bond consistency condition enables $N_{\text{As-Ga}}$ to be obtained from $N_{\text{Ga-As}}$ (for the compositions here, they are essentially equal); combining this with $N_{\text{As-X}}$ gives $N_{\text{As-As}}$. We already have the three P partial coordinations (table 1). Thus, assuming $N_{\text{Ga-Ga}} = 0$, the EXAFS data give us all the other partial coordinations. For convenience, we now calculate the mean number of bonds present in the sample from the coordinations. Neglecting a factor of N, the number of atoms in the sample, the number of i–j bonds is given by $c_i N_{i-j}$ or by $c_j N_{j-i}$ (bond consistency condition again), while the number of homonuclear i–i bonds is given by $\frac{1}{2}c_i N_{i-i}$, the factor $\frac{1}{2}$ correcting for double counting. The sum of all the bond numbers gives the mean number of bonds per atom, which is half the mean coordination.

The bond numbers, and their sum, are plotted in figure 10 where the data have been extrapolated to an assumed 3-fold coordinated a-P. The (large) uncertainties have been omitted to avoid confusing the diagram. We note that there is evidence for a tetrahedral network up to about 30–40 at.% P, with a possible decrease towards 3-fold coordination thereafter. The sharp fall in the numbers of Ga–As bonds, also evident in the infrared data, is clear. The number of Ga–P bonds rises rapidly at low P content, remains high and roughly constant over an appreciable composition range, and only falls at very high P content due to the lack of Ga atoms; this behaviour is also clearly displayed in the infrared data. There are few P–P bonds until the P content exceeds 50 at.%, and the other bonds are few at all compositions.

Attempts to explain the behaviour of the optical gap from the data in figure 10 run into difficulty at low P content. The absorption edges are all well fitted by the Tauc relation, which assumes a parabolic dependence of the conduction band (CB) and valence band (VB) densities of states (DOS) at the band edges. Also, the slopes and shapes of all the absorption edges are very similar across the composition range (B = 650–700 $\text{cm}^{-1/2}\,\text{eV}^{-1/2}$). We are therefore led to assume that the electron states at the band edges evolve by a simple replacement of Ga–As levels with Ga–P levels, without any substantial modification of the CB and VB DOS. It is therefore surprising to find that E_{opt} remains constant at a value characteristic of a-GaP over such an appreciable composition range, particularly at low P content, since one would expect the band edge DOS to be dominated

by GaAs states (giving rise to a lower band gap) until a large percentage of P results in the larger GaP band gap. Indeed, the data in figure 10 show that, for a simple bond replacement model, the increase in band gap should not take place before a P content of 30 at.%. We are therefore led to the conclusion that there is some additional mechanism involved in the band gap evolution on addition of P, possibly involving a rigid shift in the VB or CB electron levels. This, however, is unlikely to explain the sudden increase in band gap at low P content.

However, for P contents greater than 30 at.%, the optical gap data do seem to be consistent with the very simple argument, based on the idea of independent bonds, that the measured optical gap is that of the majority bond. E_{opt} remains approximately constant at 1.2 eV between about 30 at.% P and 60–70 at.% P, where Ga–P bonds are in the majority. Only at the highest P content, where the number of P–P bonds begins to exceed that of Ga–P bonds, does E_{opt} start to rise towards a value characteristic of a-P.

The dominance of Ga–P bonds over an appreciable composition range is due to the presence of chemical order in the amorphous $Ga_xAs_yP_z$ films. Almost all amorphous covalent alloys studied to date show strong chemical order. They also tend to have wide composition regions where the band gap is almost constant; examples are a-$Si_{1-x}N_x$ [10] and a-$Si_{1-x}O_x$ [16]. The results discussed here show that a-$Ga_xAs_yP_z$ films are at least partially chemically ordered.

8. Conclusions

The local structure and bonding environments around Ga, As and P atoms in sputtered a-$(GaAs)_{0.5(1-z)}P_z$ thin films ($0 \leq z \leq 0.73$) have been investigated by means of EXAFS experiments; absorption edges on all three components were measured. Values for the bond lengths, Debye–Waller factors and partial coordination numbers determined from the different absorption edges were all consistent with one another.

The bond lengths and Debye–Waller factors were found to be independent of composition. The bonding environment around Ga atoms was found to be partially chemically ordered, with Ga–P bonds favoured. Infrared data are consistent with this.

Ga and As atoms are tetrahedrally coordinated over the composition range investigated, while the total P coordination remains at 4 up to ~30 at.% P but decreases towards 3 at higher P contents. The amorphous network in the a-GaAsP films is therefore tetrahedrally bonded for P contents up to ~30 at.% but, in more P-rich films, consists of a mixture of 4-fold and 3-fold sites.

Acknowledgments

The authors wish to thank the staff at Daresbury Laboratory for their help and advice. The work as a whole was funded by the SERC.

References

[1] Thomas G and Ophey W 1990 *Phys. World* **3** December 36
[2] Theye M L, Gheorghiu A and Launois H 1980 *J. Phys. C: Solid State Phys.* **13** 6569

[3] Gheorghiu A and Theye M L 1981 *Phil. Mag.* B **44** 285
[4] Dixmier J, Gheorghiu A and Theye M L 1984 *J. Phys. C: Solid State Phys.* **17** 2271
[5] Baker S H, Manssor M I, Gurman S J, Bayliss S C and Davis E A 1992 *J. Non-Cryst. Solids* at press
[6] Manssor M I and Davis E A 1990 *J. Phys.: Condens. Matter* **2** 8063
[7] Morrell C, Campbell J C, Diakun G P, Dobson B R, Greaves G N and Hasnain S S (undated) *EXAFS Users' Manual* (Daresbury: SERC)
[8] Gurman S J, Binsted N and Ross I 1984 *J. Phys. C: Solid State Phys.* **17** 143
[9] Joyner R W, Mastin K J and Meehan P 1987 *J. Phys. C: Solid State Phys.* **20** 4005
[10] Bayliss S C and Gurman S J 1991 *J. Non-Cryst. Solids* **127** 174
[11] Greaves G N, Elliot S R and Davis E A 1979 *Adv. Phys.* **28** 49
[12] Ichikwawa T 1973 *Phys. Status Solidi* a **19** 347
[13] Sharma B D and Donohue J 1962 *Z. Krist.* **177** 293
[14] Gurman S J 1992 *J. Non-Cryst. Solids* at press
[15] Extance P 1981 *PhD Thesis* Cambridge University
[16] Singh A, Bayliss S C, Gurman S J and Davis E A 1992 *J. Non-Cryst. Solids* at press